CHAPTER-5

EXERGY ANALYSIS OF DOUBLE EFFECT H_2O–LiCl ABSORPTION REFRIGERATION SYSTEMS AND COMPARISON WITH H_2O–LiBr SYSTEMS

CHAPTER-5

EXERGY ANALYSIS OF DOUBLE EFFECT H$_2$O–LiCl ABSORPTION REFRIGERATION SYSTEMS AND COMPARISON WITH H$_2$O–LiBr SYSTEMS

5.1 Introduction

Double effect vapour absorption refrigeration systems (VARSs) with two vapour generators provide higher coefficient of performance (COP) than a single effect VARS with a single vapour generator. Double effect systems have also the advantage of better heat load management and low heat dissipation from its components to surrounding [1]. Hence, they are preferred over single and other multi effect systems for commercial use in the refrigeration industry [2–4]. But contrary to the single effect system, the flow arrangement is little complicated in the double effect systems due to presence of more number of components. The flow schematics of the double effect series, parallel and reverse parallel configurations were earlier shown and described completely in Chapter 4 and also in Chapter 1; hence these are not shown again in Chapter 5.

In Chapter 4, the detail thermodynamic analyses of the double effect H$_2$O–LiCl VARS configurations (series, parallel and reverse parallel) were provided on the basis of the first law of thermodynamics (energy analysis). In this Chapter, the series, parallel and reverse parallel flow configurations of double effect H$_2$O–LiCl absorption refrigeration systems are considered to evaluate and analyze their exergetic performances.

Exergy analysis based on second law of thermodynamics is often used as a tool for evaluating performance of thermal systems and energy conversion devices. Exergy analysis gives a better insight into the system operation and provides complete details regarding the system performance. Since, the properties of H$_2$O–LiCl salt solution are different from that of H$_2$O–LiBr, therefore the effect of operating temperatures on maximum allowable salt concentration and also on performance of double effect VARS configurations would not be the same with that of H$_2$O–LiBr systems. In order to find the complete details regarding performance of double effect H$_2$O–LiCl VARS configurations, the exergy analysis is necessary which is performed and presented in this Chapter. As pointed out earlier in Chapter 4, a new set of thermodynamic property relations [5] is considered. These property relations are valid from the crystallization

temperature up to 400 K in temperatures and also from pure water up to 50 wt% concentration of H_2O–LiCl solutions. The parametric analysis is carried out to evaluate the effects of component temperatures on exergetic performance of the series, parallel and reverse parallel flow configurations of double effect H_2O–LiCl VARS. As pointed out earlier in Chapter 4, the performance the double effect parallel and reverse parallel flow systems are dependent on the distribution ratio (D), therefore, the analysis is also done with respect to D variation for these two configurations. Further, the exergetic performances of the H_2O–LiCl based double effect series, parallel and reverse parallel systems are compared with their H_2O–LiBr counterparts under identical operating conditions. Details regarding exergetic performances of double effect H_2O–LiCl VARS configurations and their operational difference with the corresponding double effect H_2O–LiBr VARS configurations are also highlighted in this Chapter

5.2 Modelling Assumptions

The assumptions that are made for exergy analysis and the assumed parameter values are similar with what was assumed in Chapter 4 with respect to energy analysis. Cooling load is fixed 350 kW. HPG heat source is saturated steam and its saturation temperature is 10°C higher than the HPG temperature. Motor efficiency is taken as 90% while the SHE I and SHE II efficiencies are taken 75%. Water temperatures at inlet and outlet of the condenser and absorber are considered as 25°C and 30°C respectively. Evaporator inlet and outlet water temperatures are taken as 15°C and 10°C respectively. It is assumed that the systems operate under steady state without any heat loss between the system and surroundings. Pressure losses in the pipelines and heat exchangers are neglected. The refrigerant (water) is saturated liquid at condenser exit and saturated vapour at the evaporator outlet. Further, it is assumed that the absorber and evaporator operate at the same pressure. Similarly, the operating pressures of the condenser and the LPG are also assumed same. It is also assumed that the strong refrigerant solution at absorber exit is saturated liquid mixture at absorber pressure and temperature. Similarly, the medium and weak solutions at HPG and LPG exits are saturated liquid mixtures at their respective generator pressure and temperature.

5.3 Exergy based thermodynamic modelling of the double effect VARS

Calculation of thermodynamic properties of the working fluids (water and H_2O–LiCl solution) is very crucial in thermodynamic modelling of VARS. Thermodynamic properties of water in the liquid and vapour state are computed using International Associations for the Properties of Water and Steam (IAPWS) formulation 1997 [6]. Properties of H_2O–LiCl solution are calculated using the correlations of Patek and Klomfar [5]. The medium solution concentration at the HPG exit (X_8) is calculated in an iterative manner satisfying energy balance in the LPG [2]. Value of X_8 depends on pressure and temperature in the VARS components (LPG, HPG, evaporator, absorber and the condenser). First, the strong and weak solution concentrations (X_4 and X_{15}) at absorber and LPG exit are calculated from known pressure and temperature in these components. This is again done in an iterative manner using a specific set of equations (chemical potential) given in Ref. [5]. Calculation of X_8 and the HPG temperature (T_{HPG}) which is an input parameter, helps in determination of HPG pressure from correlations given in Ref. [5]. Details were given in the Appendix of this thesis. The mass and energy balance equations applied in modelling the double effect VARS configurations were described in detail in the previous Chapter (4), hence these are not repeated in this Chapter. The following general exergy balance equation is used to calculate exergy destruction (or irreversibility) in various components of the double effect series, parallel and reverse parallel systems.

$$\sum \dot{Ex}_{in} - \sum \dot{Ex}_{out} + \dot{Q}\left(1 - \frac{T_0}{T}\right) - \dot{W} - \dot{Ex}_d = 0 \tag{5.1}$$

The exergy efficiency of the double effect series, parallel and reverse parallel system is estimated using following equation:

$$\eta = \frac{\dot{Ex}_{w,E_{out}} - \dot{Ex}_{w,E_{in}}}{\dot{Ex}_{s,HPG_{in}} - \dot{Ex}_{s,HPG_{out}} + \sum \dot{W}_{SP}} \tag{5.2}$$

where, $\dot{Ex}$ is the total exergy, the product of mass flow rate and specific exergy. The total system irreversibility $\left(\dot{I}_{tot}\right)$ is determined by summing up the exergy

destruction i.e. $\dot{Ex}_d$ (or irreversibility $\dot{I}$) occurring in the system components of a given flow configuration.

5.4 A brief summary of results presented in Chapter 4

The energy based parametric analysis of the double effect H_2O–LiCl VARS configurations was presented in Chapter 4 of this study where the variations of COP, component heat loads, pumping power, solution concentrations (weak, medium and strong) and pressure were shown with respect to (i) simultaneous change in both T_{HPG} and T_{LPG} (ii) change in T_{HPG} at fixed T_{LPG} and (iii) change in T_{LPG} at fixed T_{HPG}. The energetic performance variations were shown for all the three double effect VARS configurations with respect to four different cases of fixed condenser and absorber and evaporator temperatures viz. Case 1: $T_C = T_A = $ 33°C and $T_E = $ 8°C, Case 2: $T_C = T_A$ =35°C and T_E =8°C, Case 3: $T_C = T_A$ =38°C and T_E =8°C and Case 4: $T_C = T_A$ =35°C and T_E =5°C. The distribution ratio (D) was also varied to evaluate its effect on first law performance of the double effect parallel and reverse parallel systems and to find the optimum D through parametric variation of T_{LPG} and T_{HPG} for the above four cases and also for an additional case (Case 5: $T_C = T_A$ =33°C and T_E =5°C). The upper limit of T_{LPG} in all the double effect H_2O–LiCl VARS configurations and the D value additionally in the parallel and reverse parallel systems were determined such that the maximum H_2O–LiCl solution concentration is always within 50 wt% limit. The upper T_{LPG} limits for the series, parallel and reverse parallel configurations were found (i) 71°C, 69°C and 63°C respectively during Case 1, (ii) 73°C, 71°C and 67°C during Case 2 (iii) 76°C, 75°C and 73°C during Case 3 and (iv) 73°C, 72°C and 70°C during Case 4. Accordingly, for a given case of fixed T_C, T_A and T_E, corresponding to maximum COP, the optimum values of T_{LPG}, T_{HPG} and D were determined through parametric variation. The upper T_{LPG} limits stated above are also the optimal T_{LPG} values corresponding to maximum COP. Similarly the optimal T_{HPG} values corresponding to maximum COP for the series, parallel and reverse parallel configurations were respectively as follows: (i) 105°C, 106°C and 102°C for Case 1 (ii) 109°C, 109°C and 108°C for Case 2 (iii) 116°C, 116°C and 115°C for Case 3 and (iv) 112°C, 113°C and 112°C for Case 4. The optimal D values

corresponding to maximum COP were found to be 0.5 for the parallel and reverse parallel systems during all the cases except for the reverse parallel system during Case 3 and Case 4 where D was 0.5 and 0.65 respectively. During Case 1, the maximum COP values obtained from the series, parallel and reverse parallel configurations were found 1.428, 1.469 and 1.406 respectively. Similarly, the maximum COP values of the three double effect VARS configurations corresponding to Case 2 were 1.369, 1.411 and 1.347. During Case 3, the maximum COP values for the three double effect VARS configurations were 1.207, 1.273 and 1.209 and during Case 4, the corresponding maximum COP values were 1.208, 1.270 and 1.185 respectively. As such, for a given, the maximum COP was the highest for the parallel configuration followed by that of the series and reverse parallel. Further, highest maximum COP values in all the three VARS configurations were found during Case 1.

Additionally, a performance comparison in terms of COP, HPG heat load, SP power and solution concentrations (X_8 and X_{15}) and HPG pressure was also provided between the double effect H_2O–LiCl and H_2O–LiBr systems under identical conditions of component temperatures. It was found that under identical conditions, H_2O–LiCl operated double effect systems perform better in terms of COP than the corresponding H_2O–LiBr systems relatively at lower T_{LPG} and T_{HPG}. It was also observed that, the COP difference between H_2O–LiCl and H_2O–LiBr operated double effect systems which is relatively more at lower T_{LPG} and T_{HPG}, gradually decreases with increase in T_{LPG} and T_{HPG}. Further, maximum COP difference was observed in the reverse parallel configuration.

The above observations were however made based on energy analysis of the double effect VARS configurations. Energy analysis provides only a quantitative measurement of energy balance in the VARS components in finding the first law based performance parameter i.e. the COP. It does not give any idea about the source of inefficiency and irreversible losses occurring in various system components. It is exergy which assigns quality to energy of a system at a given state and thus provides the theoretical base for evaluating the irreversible losses and the second law efficiency of any thermal system and in this case the double effect VARS configurations. The exergy based results are presented in the following sections.

5.5 Exergy based results and discussion

In exergy analysis, first the exergy of the flow stream is calculated at each and every state of the cycle along with the exergy associated with the heat and work transfer terms. Next, from the basic definition, the exergy efficiency (a second law based performance parameter) of the overall system is calculated. And finally the exergy balance equation is applied for calculating exergy destruction (irreversibility) in each system component. Exergetic performance is subject to vary with heat source and components' operating temperatures. The results obtained from exergy analysis of the three double effect H_2O–LiCl VARS configurations are presented in this section in a similar manner as it was presented for energy analysis in Chapter 4. Like in Chapter 4, here in this Chapter also, the exergetic performance variations (mainly the exergy efficiency and irreversibility variations) are shown with respect to (i) simultaneous change in T_{HPG} and T_{LPG} (ii) change in T_{HPG} at fixed T_{LPG} (iii) change in T_{LPG} at fixed T_{HPG} and (iv) change in D of the parallel and reverse parallel systems for various cases of fixed condenser, absorber and evaporator temperatures. Further, the exergetic performances of the H_2O–LiCl based double effect series, parallel and reverse parallel systems are compared with their H_2O–LiBr counterparts under identical operating conditions for Case 1 at $T_C = T_A$=33°C and T_E=8°C.

5.5.1 Effect of HPG temperature (T_{HPG}) on exergetic performances of double effect H_2O–LiCl VARS configurations

The effect of T_{HPG} change on exergy efficiency is shown in Fig. 5.1a and Fig. 5.1b for three different absorber and condenser temperatures (33°C, 35°C and 38°C) and two different evaporator temperatures (T_E=5°C and T_E=8°C). Fig. 5.1a corresponds to T_{HPG} variation with simultaneous change in T_{LPG} while in Fig. 5.1b, T_{HPG} variation is shown for fixed T_{LPG} values with T_{LPG} fixed at their respective upper limits. The other simulation conditions which were presented in detail in Chapter 4 are also taken same here in this Chapter of this study. These are shown in tabular form in Table 5.1. It was mentioned in Chapter 4 that the decision regarding this simultaneous T_{HPG} and T_{LPG} change and also fixed T_{LPG} during T_{HPG} variation was taken after lot of maneuvering with the computer simulation programs to finally arrive at the optimal temperature

difference in various cases. It was actually the upper bound of T_{LPG} that posed a limit on the maximum solution concentration at certain fixed values of T_C, T_A and T_E. Further, lowering of T_{HPG} below certain limit was also not possible due to some unrealistic results that were obtained with violation of mass balance in the systems.

From Fig. 5.1a, it is seen that the exergy efficiency increases with increase in both T_{HPG} and T_{LPG} for all the three double effect VARS configurations at fixed other component temperatures.
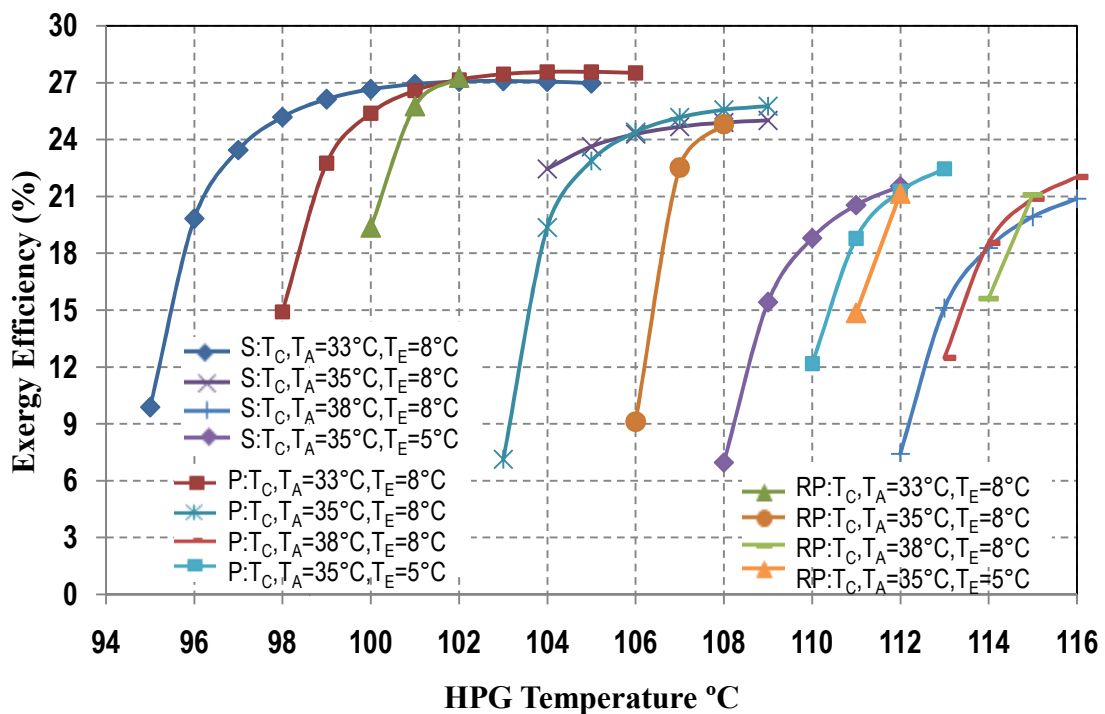
Fig. 5.1a: Exergy efficiency variation with simultaneous change in T_{HPG} and T_{LPG} for the series, parallel and reverse parallel configurations with $T_{HPG} - T_{LPG}$ differences of (i) 34°C, 37°C and 39°C during Case 1, (ii) 36°C, 38°C and 41°C during Case 2 (iii) 40°C, 41°C and 42°C during Case 3 and (iv) 39°C, 41°C and 42°C during Case 4
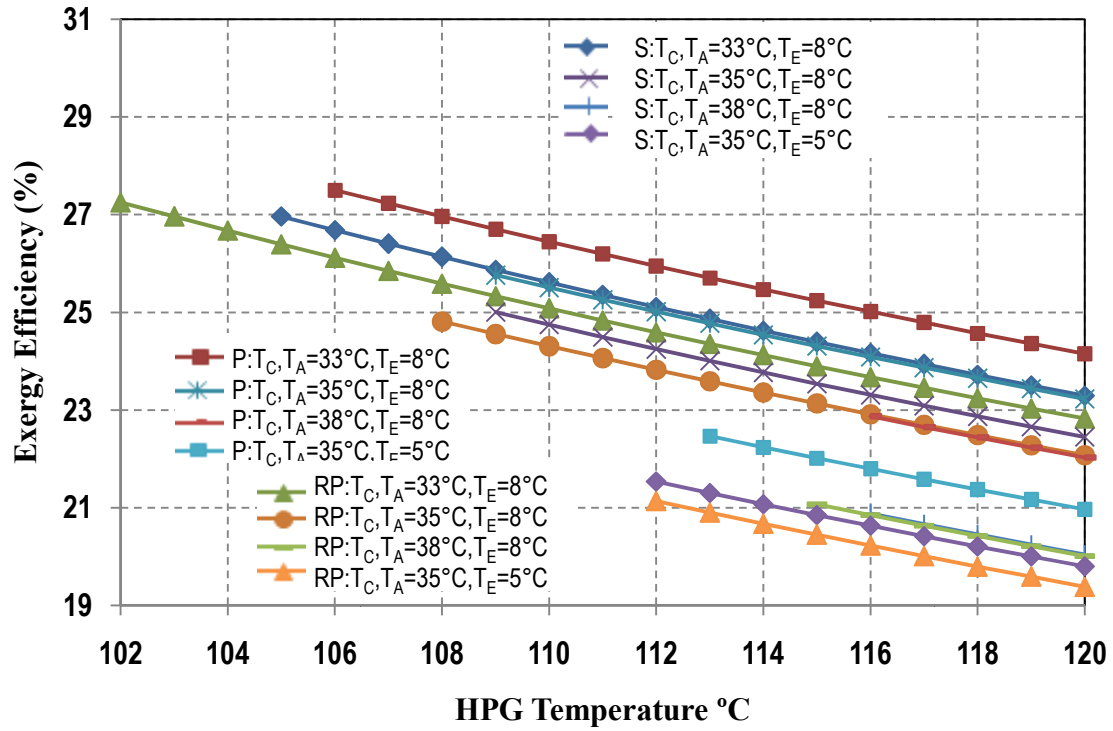
Fig. 5.1b: Exergy efficiency variation with T_{HPG} at fixed T_{LPG} for the series, parallel and reverse parallel configurations respectively [T_{LPG} fixed at (i) 71°C, 69°C and 63°C during Case 1, (ii) 73°C, 71°C and 67°C during Case 2 (iii) 76°C, 75°C and 73°C during Case 3 (iv) 73°C, 72°C and 70°C during Case 4]

Table 5.1: Selected range of T_{HPG} and difference between T_{HPG} and T_{LPG} used in simulation

Case	Series		Parallel		Reverse Parallel	
	T_{HPG} Range	$T_{HPG} - T_{LPG}$	T_{HPG} Range	$T_{HPG} - T_{LPG}$	T_{HPG} Range	$T_{HPG} - T_{LPG}$
$T_C = T_A = 33°C$, $T_E = 8°C$	95–105°C	34°C	98–106°C	37°C	100–102°C	39°C
$T_C = T_A = 35°C$, $T_E = 8°C$	104–109°C	36°C	103–109°C	38°C	106–108°C	41°C
$T_C = T_A = 38°C$, $T_E = 8°C$	112–116°C	40°C	113–116°C	41°C	114–115°C	42°C
$T_C = T_A = 35°C$, $T_E = 5°C$	108–112°C	39°C	110–113°C	41°C	111–112°C	42°C

Earlier, in Chapter 4, it was reported that the maximum COP in the series configuration is 1.428 and it was obtained at T_{HPG} =105°C and T_{LPG} =71°C for Case 1 at fixed $T_C = T_A$ =33°C and T_E =8°C. However, from the present exergy analysis, it is found that the exergy efficiency for the series configuration is the maximum at T_{HPG} =103°C and T_{LPG} =69°C for Case 1 and the maximum exergy efficiency is found to be 29.26%. Increase in T_{HPG} beyond 103°C in the series configuration causes slight decrease in exergy efficiency. This is more clearly depicted in Fig. 5.1b with almost a similar trend of variation in all the three systems. What is seen from Figs. 5.1a and 5.1b is that for each system, there exists an optimal combination of T_{HPG} and T_{LPG} at which, earlier the COP in Chapter 4 and now the exergy efficiency is also the maximum. The trend of exergy efficiency variation shown in Fig. 5.1a with respect to simultaneous T_{HPG} and T_{LPG} change for the series configuration, although looks similar to the corresponding COP variation reported in Chapter 4, but the difference is that the maximum exergy efficiency is obtained at T_{HPG} and T_{LPG} values 2°C less than those corresponding to maximum COP for the series configuration with respect to Case 1. The COP value at T_{HPG} =103°C and T_{LPG} =69°C is 1.41 and it is slightly lower than the maximum COP (1.428). In the parallel configuration, the maximum exergy efficiency for Case 1 is 27.56% (refer Fig. 5.1a) and this is obtained at T_{HPG} =105°C and T_{LPG} =68°C while the maximum COP (1.469) was actually obtained at T_{HPG} =106°C and T_{LPG} =69°C (refer Chapter 4). However, in the other cases of fixed component temperatures (Case 2, Case 3 and Case 4), the values of T_{HPG} and T_{LPG} corresponding to maximum COP and maximum exergy efficiency are the same in all the three double effect H_2O–LiCl VARS configurations.

Regarding the slight mismatch in T_{HPG} and T_{LPG} values corresponding to maximum COP and maximum exergy efficiency (also minimum irreversibility) in the series and parallel configurations at Case 1, either of the two conditions be selected depending on criteria based on the maximum exergy efficiency (or minimum total irreversibility) or the maximum COP. However, it was found that the COP value in the series configuration at conditions of maximum exergy efficiency is 1.26% less compared to 0.434% increase in exergy efficiency and 0.738% reduction in total irreversibly from

condition of maximum COP. Similarly, in the parallel system also, the percentage reduction in COP (0.633%) is more compared to exergy efficiency increase of 0.214% and total irreversibly reduction of 0.266%. Therefore, the condition of maximum COP be preferred for this Case 1 where T_{HPG} and T_{LPG} combinations were little different for maximum COP and maximum exergy efficiency (also minimum irreversibility).

The total system irreversibility variations of the three systems under various cases of fixed component temperatures with respect to (i) simultaneous T_{HPG} and T_{LPG} change and (ii) change in T_{HPG} at fixed T_{LPG} are shown in Figs. 5.2a and 5.2b respectively. From Fig. 5.2a, it is seen that the total system irreversibility decreases in all the three double effect H_2O–LiCl systems with simultaneous increase in T_{HPG} and T_{LPG} and for Case 1, the irreversibility is the minimum (36.32 kW) at T_{HPG} =103°C and T_{LPG} =69°C in the series configuration. In the parallel configuration, the total system irreversibility is the minimum at T_{HPG} =105°C and T_{LPG} =68°C for Case 1 with a corresponding minimum irreversibility value of 35.35 kW. Further increase in T_{HPG} (with T_{LPG} fixed at its limiting value) causes irreversibility increase in all the three systems under various cases of fixed component temperatures. This is clearly depicted in Fig. 5.2b. In the reverse parallel configuration, for Case 1, the maximum COP (1.406) which was obtained at T_{HPG} =102°C and T_{LPG} =63°C and now in the present analysis too, the maximum exergy efficiency (27.25%) and minimum total system irreversibility (34.87 kW) are found at the same T_{HPG} and T_{LPG} (see Figs. 5.1a and 5.2a). Further it is observed that T_{HPG} and T_{LPG} values corresponding to maximum exergy efficiency and minimum total system irreversibility are the same in all the systems under various cases of fixed component temperatures. The component wise irreversibility distribution in various system components of the series, parallel and reverse parallel systems with simultaneous change in T_{HPG} and T_{LPG} is shown in Table 5.2 (a–b) for Case 1 at fixed $T_C = T_A$=33°C, T_E=8°C. That the irreversibility in various system components decreases with simultaneous increase in T_{HPG} and T_{LPG} is evident from the results in Table 5.2 (a–b).
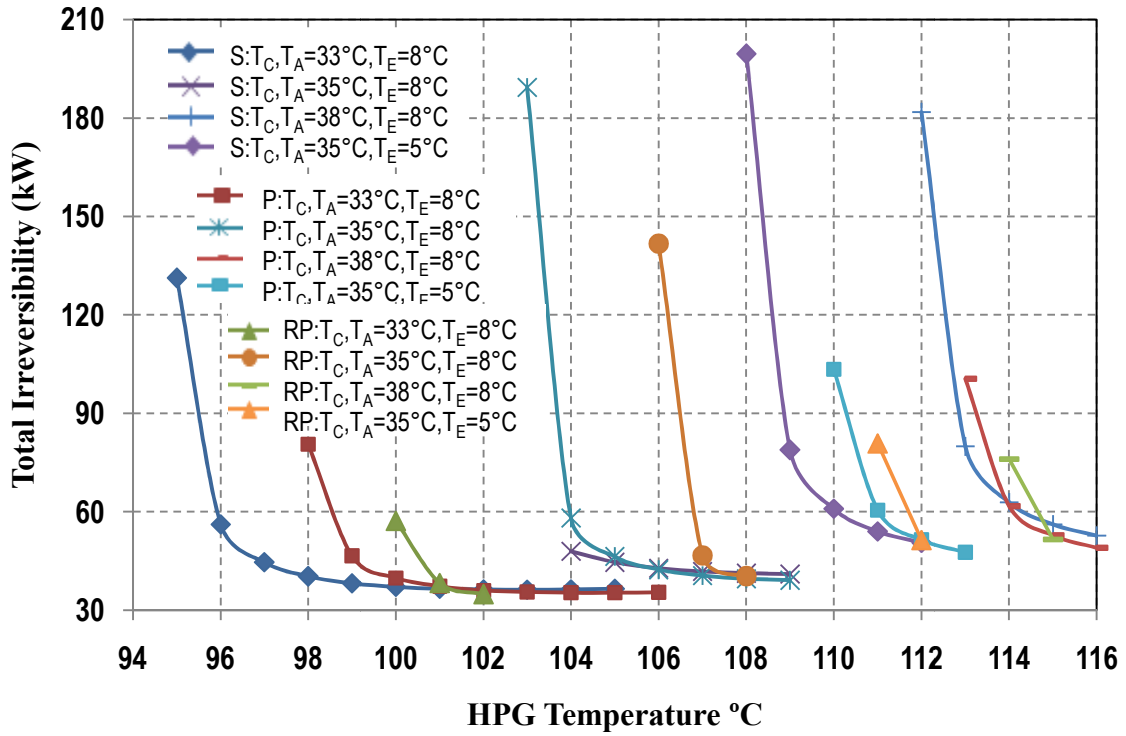
Fig. 5.2a: Total irreversibility variation with simultaneous change in T_{HPG} and T_{LPG} respectively for the series, parallel and reverse parallel configurations with $T_{HPG} - T_{LPG}$ differences of (i) 34°C, 37°C and 39°C during Case 1, (ii) 36°C, 38°C and 41°C during Case 2 (iii) 40°C, 41°C and 42°C during Case 3 and (iv) 39°C, 41°C and 42°C during Case 4
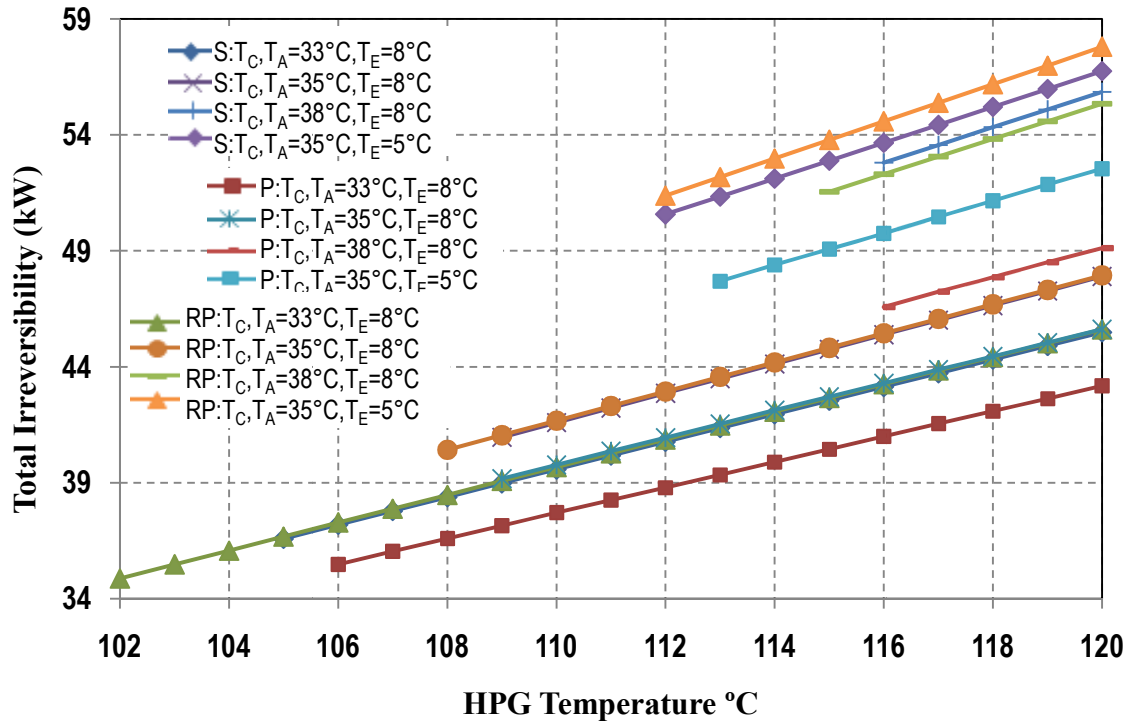
Fig. 5.2b: Total irreversibility variation with T_{HPG} at fixed T_{LPG} for the series, parallel and reverse parallel configurations respectively [T_{LPG} fixed at (i) 71°C, 69°C and 63°C during Case 1, (ii) 73°C, 71°C and 67°C during Case 2 (iii) 76°C, 75°C and 73°C during Case 3 (iv) 73°C, 72°C and 70°C during Case 4]

Table 5.2a: Component wise irreversibility (in kW) variation with simultaneous change in T_{HPG} and T_{LPG} for Case 1 at fixed $T_C = T_A = 33°C$, $T_E = 8°C$ (Series)

T_{HPG}	$\dot{I}_{HPG}$	$\dot{I}_{LPG}$	$\dot{I}_C$	$\dot{I}_E$	$\dot{I}_A$	$\dot{I}_{SHE1}$	$\dot{I}_{SHE2}$	$\dot{I}_{ExV1}$	$\dot{I}_{ExV2}$	$\dot{I}_{ExV3}$	$\dot{I}_{ExV4}$	$\dot{I}_{ExV5}$	$\dot{I}_{SP1}$	$\dot{I}_{SP2}$
Series: $T_C = T_A = 33°C,\ T_E = 8°C$														
95	23.28	1.53	4.83	5.84	18.58	25.98	49.07	0.69	0.27	0.38	0.45	-	0.33	-
96	10.21	1.57	3.76	5.84	11.09	7.87	14.33	0.69	0.43	0.21	0.08	-	0.09	-
97	8.22	1.39	3.60	5.84	10.56	4.99	8.79	0.69	0.47	0.01	0.07	-	0.05	-
98	7.49	0.96	3.54	5.84	10.60	3.82	6.54	0.69	0.49	0.01	0.32	-	0.04	-
99	7.15	1.09	3.52	5.84	10.88	3.20	5.33	0.69	0.51	0.01	0.03	-	0.03	-
100	6.99	0.93	3.50	5.84	11.25	2.81	4.58	0.69	0.53	0.01	0.03	-	0.03	-
101	6.91	0.77	3.50	5.84	11.66	2.55	4.07	0.69	0.55	0.03	0.03	-	0.02	-
102	6.89	0.63	3.50	5.84	12.13	2.37	3.71	0.69	0.56	0.01	0.02	-	0.02	-
103	6.91	0.49	3.50	5.84	12.55	2.24	3.44	0.69	0.58	0.06	0.03	-	0.02	-
104	6.94	0.31	3.51	5.84	13.06	2.13	3.23	0.69	0.59	0.01	0.07	-	0.02	-
105	7.00	0.24	3.52	5.84	13.52	2.06	3.07	0.69	0.61	0.03	0.02	-	0.01	-

Table 5.2b: Component wise irreversibility (in kW) variation with simultaneous change in T_{HPG} and T_{LPG} for Case 1 at fixed $T_C = T_A = 33°C$, $T_E = 8°C$ (Parallel and Reverse Parallel)

T_{HPG}	$\dot{I}_{HPG}$	$\dot{I}_{LPG}$	$\dot{I}_{C}$	$\dot{I}_{E}$	$\dot{I}_{A}$	$\dot{I}_{SHE1}$	$\dot{I}_{SHE2}$	$\dot{I}_{ExV1}$	$\dot{I}_{ExV2}$	$\dot{I}_{ExV3}$	$\dot{I}_{ExV4}$	$\dot{I}_{ExV5}$	$\dot{I}_{SP1}$	$\dot{I}_{SP2}$
Parallel: $T_C = T_A = 33°C$, $T_E = 8°C$														
98	13.01	4.44	2.48	5.84	15.97	20.24	17.03	0.69	0.68	0.06	0.13	0.10	0.01	-
99	8.17	3.15	3.05	5.84	11.10	7.45	6.44	0.69	0.58	0.04	0.01	0.04	0.00	-
100	7.39	2.57	3.18	5.84	10.64	4.81	4.20	0.69	0.56	0.01	0.02	0.02	0.00	-
101	7.23	2.11	3.25	5.84	10.75	3.64	3.23	0.69	0.54	0.01	0.02	0.01	0.00	-
102	7.29	1.70	3.29	5.84	11.09	2.98	2.69	0.69	0.53	0.01	0.01	0.01	0.00	-
103	7.46	1.29	3.32	5.84	11.54	2.56	2.35	0.69	0.51	0.00	0.01	0.01	0.00	-
104	7.69	0.87	3.34	5.84	12.02	2.27	2.11	0.69	0.50	0.00	0.01	0.01	0.00	-
105	7.97	0.46	3.36	5.84	12.53	2.06	1.94	0.69	0.49	0.00	0.01	0.01	0.00	-
106	8.29	0.03	3.38	5.84	13.05	1.90	1.81	0.69	0.47	0.00	0.01	0.01	0.00	-
Reverse Parallel: $T_C = T_A = 33°C$, $T_E = 8°C$														
100	5.73	4.48	2.66	5.84	12.82	12.69	11.62	0.69	0.68	0.00	0.00	-	0.03	0.01
101	2.90	2.15	3.10	5.84	10.80	4.56	7.78	0.69	0.52	0.00	0.00	-	0.01	0.00
102	2.92	0.19	3.19	5.84	11.48	2.96	7.19	0.69	0.41	0.00	0.00	-	0.01	0.00

From the irreversibility results in Table 5.2 (a–b), it is also observed that the order in which the system components contribute to total system irreversibility change with simultaneous increase in T_{HPG} and T_{LPG}. Say for example, for Case 1 in the series configuration at T_{HPG} = 95°C and T_{LPG} =61°C, the SHE II, SHE I, HPG, absorber, evaporator, condenser and the LPG are the components in sequential order with their respective highest contribution to the total system irreversibility. However at higher T_{HPG} and T_{LPG}, the order of the components in terms of their contribution to total system irreversibility changes. Since evaporator irreversibility does not change, so at T_{HPG} = 105°C ($T_{LPG} = T_{HPG} -34$), the evaporator irreversibility is the highest followed by the irreversibility contributions of the absorber, HPG, condenser, SHE II, SHE I and the LPG. This trend of irreversibility contribution of the components to total irreversibility is more or less similar in the other two systems (parallel and reverse parallel) at higher T_{HPG} and T_{LPG}. At lower T_{HPG} and T_{LPG} however, the order in which the components contribute to total system irreversibility changes and is little different from that of the series configuration.

The irreversible losses occurring in various system components during T_{HPG} change (with T_{LPG} fixed at its limiting value) are shown in Table 5.3a, Table 5.3b and Table 5.3c for Case 1 at fixed $T_C = T_A$=33°C, T_E=8°C. That the component irreversible losses are the minimum at their corresponding optimum T_{HPG} and T_{LPG} and increase further with T_{HPG} is visible from the results shown in Table 5.2a, Table 5.2b, Table 5.3a, Table 5.3b and Table 5.3c. The irreversible loss in the evaporator is not affected by T_{HPG} and T_{LPG} variation and irreversible losses are also the minimum and negligible in the expansion valves and also in the SPs.

The exergy efficiency and total system irreversibility variation with (i) simultaneous change in T_{HPG} and T_{LPG} (Figs. 5.1a and 5.2a) and (ii) change in T_{HPG} at fixed T_{LPG} (Figs. 5.1b and 5.2b) is more or less similar for the other cases of fixed component temperatures in all the three double effect H₂O–LiCl VARS configurations. Like COP, exergy efficiency also decreases with increase in absorber and condenser temperatures.

206

Table 5.3a: Component wise irreversibility (in kW) variation with T_{HPG} (fixed T_{LPG}) in the double effect series systems for Case 1 ($T_C = T_A$ =33°C, T_E =8°C)

T_{HPG}	$\dot{I}_{HPG}$	$\dot{I}_{LPG}$	$\dot{I}_C$	$\dot{I}_E$	$\dot{I}_A$	$\dot{I}_{SHE1}$	$\dot{I}_{SHE2}$	$\dot{I}_{ExV1}$	$\dot{I}_{ExV2}$	$\dot{I}_{ExV3}$	$\dot{I}_{ExV4}$	$\dot{I}_{ExV5}$	$\dot{I}_{SP1}$	$\dot{I}_{SP2}$
Series: T_{LPG} =71°C, $T_C = T_A$=33°C and T_E=8°C														
105	7.00	0.24	3.52	5.84	13.52	2.06	3.07	0.69	0.61	0.03	0.02	-	0.01	-
106	7.00	0.68	3.53	5.84	13.52	2.06	3.19	0.69	0.64	0.03	0.02	-	0.01	-
107	7.01	1.11	3.54	5.84	13.52	2.06	3.30	0.69	0.67	0.03	0.02	-	0.01	-
108	7.01	1.53	3.55	5.84	13.52	2.06	3.42	0.69	0.70	0.03	0.04	-	0.01	-
109	7.02	1.97	3.55	5.84	13.52	2.06	3.54	0.69	0.73	0.03	0.02	-	0.01	-
110	7.03	2.36	3.56	5.84	13.52	2.06	3.66	0.69	0.77	0.03	0.06	-	0.01	-
111	7.03	2.82	3.57	5.84	13.52	2.06	3.79	0.69	0.80	0.03	0.03	-	0.01	-
112	7.04	3.23	3.58	5.84	13.52	2.06	3.91	0.69	0.83	0.03	0.04	-	0.01	-
113	7.05	3.65	3.59	5.84	13.52	2.06	4.03	0.69	0.87	0.03	0.03	-	0.01	-
114	7.06	3.98	3.60	5.84	13.52	2.06	4.16	0.69	0.90	0.03	0.12	-	0.01	-
115	7.06	4.48	3.61	5.84	13.52	2.06	4.29	0.69	0.94	0.03	0.03	-	0.01	-
116	7.07	4.87	3.62	5.84	13.52	2.06	4.42	0.69	0.98	0.03	0.05	-	0.01	-
117	7.08	5.28	3.63	5.84	13.52	2.06	4.55	0.69	1.01	0.03	0.03	-	0.01	-
118	7.09	5.64	3.63	5.84	13.52	2.06	4.68	0.69	1.05	0.03	0.07	-	0.01	-
119	7.10	6.08	3.64	5.84	13.52	2.06	4.82	0.69	1.09	0.03	0.04	-	0.01	-
120	7.11	6.46	3.65	5.84	13.52	2.06	4.95	0.69	1.13	0.03	0.05	-	0.01	-

Table 5.3b: Component wise irreversibility (in kW) variation with T_{HPG} (fixed T_{LPG}) in the double effect parallel systems for Case 1 ($T_C = T_A$ =33°C, T_E =8°C)

T_{HPG}	$\dot{I}_{HPG}$	$\dot{I}_{LPG}$	$\dot{I}_C$	$\dot{I}_E$	$\dot{I}_A$	$\dot{I}_{SHE1}$	$\dot{I}_{SHE2}$	$\dot{I}_{ExV1}$	$\dot{I}_{ExV2}$	$\dot{I}_{ExV3}$	$\dot{I}_{ExV4}$	$\dot{I}_{ExV5}$	$\dot{I}_{SP1}$	$\dot{I}_{SP2}$
Parallel: T_{LPG} =69°C, $T_C = T_A$ =33°C and T_E =8°C														
106	8.29	0.03	3.38	5.84	13.05	1.90	1.81	0.69	0.47	0.00	0.01	0.01	0.00	-
107	8.28	0.48	3.38	5.84	13.05	1.92	1.86	0.69	0.50	0.01	0.01	0.01	0.00	-
108	8.28	0.93	3.39	5.84	13.06	1.94	1.92	0.69	0.53	0.01	0.01	0.01	0.00	-
109	8.28	1.37	3.39	5.84	13.06	1.95	1.98	0.69	0.56	0.01	0.01	0.01	0.00	-
110	8.27	1.81	3.40	5.84	13.06	1.97	2.04	0.69	0.59	0.01	0.01	0.01	0.00	-
111	8.27	2.26	3.40	5.84	13.07	1.99	2.10	0.69	0.62	0.01	0.01	0.01	0.00	-
112	8.27	2.69	3.41	5.84	13.08	2.00	2.16	0.69	0.65	0.00	0.00	0.01	0.00	-
113	8.27	3.13	3.41	5.84	13.09	2.02	2.22	0.69	0.68	0.00	0.01	0.01	0.00	-
114	8.27	3.56	3.42	5.84	13.09	2.03	2.28	0.69	0.71	0.00	0.01	0.01	0.00	-
115	8.27	3.98	3.42	5.84	13.09	2.05	2.34	0.69	0.74	0.00	0.01	0.01	0.00	-
116	8.27	4.41	3.43	5.84	13.10	2.07	2.41	0.69	0.77	0.00	0.01	0.01	0.00	-
117	8.27	4.83	3.43	5.84	13.10	2.09	2.47	0.69	0.81	0.00	0.01	0.01	0.00	-
118	8.27	5.25	3.44	5.84	13.11	2.10	2.53	0.69	0.84	0.00	0.01	0.01	0.00	-
119	8.27	5.67	3.44	5.84	13.11	2.12	2.60	0.69	0.88	0.00	0.01	0.01	0.00	-
120	8.27	6.08	3.45	5.84	13.11	2.14	2.66	0.69	0.91	0.00	0.01	0.01	0.00	-

Table 5.3c: Component wise irreversibility (in kW) variation with T_{HPG} (fixed T_{LPG}) in the double effect reverse parallel system for Case 1

$(T_C = T_A = 33°C,\ T_E = 8°C)$

T_{HPG}	$\dot{I}_{HPG}$	$\dot{I}_{LPG}$	$\dot{I}_C$	$\dot{I}_E$	$\dot{I}_A$	$\dot{I}_{SHE1}$	$\dot{I}_{SHE2}$	$\dot{I}_{ExV1}$	$\dot{I}_{ExV2}$	$\dot{I}_{ExV3}$	$\dot{I}_{ExV4}$	$\dot{I}_{ExV5}$	$\dot{I}_{SP1}$	$\dot{I}_{SP2}$
Reverse Parallel: T_{LPG} =63°C, T_C = T_A =33°C and T_E =8°C														
102	2.92	0.19	3.19	5.84	11.48	2.96	7.19	0.69	0.41	0.00	0.00	-	0.01	0.00
103	2.94	0.66	3.20	5.84	11.48	2.98	7.24	0.69	0.44	0.00	0.00	-	0.01	0.00
104	2.97	1.13	3.21	5.84	11.49	3.00	7.30	0.69	0.46	0.00	0.00	-	0.01	0.00
105	2.99	1.60	3.21	5.84	11.49	3.02	7.35	0.69	0.49	0.00	0.00	-	0.01	0.00
106	3.02	2.06	3.22	5.84	11.49	3.04	7.40	0.69	0.52	0.00	0.00	-	0.01	0.00
107	3.04	2.52	3.23	5.84	11.50	3.06	7.46	0.69	0.55	0.00	0.00	-	0.01	0.00
108	3.07	2.97	3.23	5.84	11.50	3.08	7.51	0.69	0.57	0.00	0.00	-	0.01	0.00
109	3.10	3.43	3.24	5.84	11.51	3.10	7.57	0.69	0.60	0.00	0.00	-	0.01	0.00
110	3.12	3.88	3.25	5.84	11.51	3.12	7.63	0.69	0.64	0.00	0.00	-	0.01	0.00
111	3.15	4.32	3.25	5.84	11.51	3.14	7.69	0.69	0.67	0.00	0.00	-	0.01	0.00
112	3.18	4.77	3.26	5.84	11.52	3.16	7.76	0.69	0.70	0.00	0.00	-	0.01	0.00
113	3.21	5.21	3.27	5.84	11.52	3.18	7.82	0.69	0.73	0.00	0.00	-	0.01	0.00
114	3.24	5.64	3.27	5.84	11.53	3.20	7.88	0.69	0.76	0.00	0.00	-	0.01	0.00
115	3.27	6.07	3.28	5.84	11.53	3.22	7.95	0.69	0.80	0.00	0.00	-	0.01	0.00
116	3.30	6.51	3.29	5.84	11.53	3.24	8.02	0.69	0.83	0.00	0.00	-	0.01	0.00
117	3.33	6.93	3.29	5.84	11.54	3.26	8.09	0.69	0.87	0.00	0.00	-	0.01	0.00
118	3.35	7.36	3.30	5.84	11.54	3.29	8.16	0.69	0.91	0.00	0.00	-	0.01	0.00
119	3.38	7.78	3.31	5.84	11.54	3.31	8.23	0.69	0.94	0.00	0.00	-	0.01	0.00
120	3.42	8.20	3.31	5.84	11.55	3.33	8.30	0.69	0.98	0.00	0.00	-	0.01	0.00

The total system irreversibility is also more at higher absorber and condenser temperatures.

Exergetic performance comparison of the double effects systems at fixed $T_C = T_A$ =35°C and at two different evaporator temperatures (T_E =5°C and T_E =5°C) shows better performance with higher exergy efficiency and lower total system irreversibility at T_E =8°C than at T_E =5°C.

Earlier in Chapter 4, it was found that the maximum COPs obtained for the four various cases of fixed absorber, condenser and evaporator temperatures was the highest for the double effect parallel configuration followed by those of the series and reverse parallel configurations. At $T_C = T_A$ =38°C and T_E =8°C, however the maximum COP obtained for the reverse parallel configuration was slightly higher than that of the series configuration. From the exergy analysis also now it is found that the maximum exergy efficiency is the highest for the parallel configuration in all the four test cases. For Case 2 and Case 4, the maximum exergy efficiency values obtained for the series configuration are higher than those obtained for the reverse parallel system while this scenario is just the reverse for Case 1 and Case 3. The parallel VARS configuration also produces the minimum total irreversibility among all the three systems at four different cases except in Case 1, where the minimum total irreversibility is observed in the reverse parallel configuration. The maximum exergy efficiencies and minimum total irreversibility values obtained for the series, parallel and reverse parallel double effect systems under various test cases are shown in Table 5.4 along with the maximum COPs. From the results in Table 5.4, it is also seen that the results corresponding to Case 1 are better than those of the other three cases.

Thus, it is seen that some of the facts regarding thermodynamic performances of the double effect VARS configurations which could not be observed very clearly from the energy analysis in Chapter 4 in terms of irreversible losses and exergy efficiency, now has been completely depicted with the help of the exergy analysis in this Chapter. Say for example, during Case 1 at $T_C = T_A$ =33°C and T_E =8°C, the highest COP was found for the parallel configuration followed by the series and reverse parallel (refer

Table 5.4). Thus, the COP was slightly higher for the series configuration than that of the reverse parallel.

Table 5.4: Maximum COP, maximum exergy efficiency and minimum total system irreversibility obtained for the double effect H_2O–$LiCl$ systems in various test cases

Cases	Series			Parallel			Reverse Parallel		
	COP (max)	η (%) (max)	$\dot{I}_{tot}$ (kW) (min)	COP (max)	η (%) (max)	$\dot{I}_{tot}$ (kW) (min)	COP (max)	η (%) (max)	$\dot{I}_{tot}$ (kW) (min)
$T_C=T_A=$ 33°C, $T_E=$ 8°C	1.428	26.96	36.59	1.469	27.50	35.48	1.406	27.25	34.87
$T_C=T_A=$ 35°C, $T_E=$ 8°C	1.369	25.00	41.04	1.411	25.76	39.18	1.347	24.81	40.42
$T_C=T_A=$ 38°C, $T_E=$ 8°C	1.207	20.88	52.80	1.273	22.02	49.08	1.209	21.07	51.55
$T_C=T_A=$ 35°C, $T_E=$ 5°C	1.208	21.54	50.57	1.270	22.47	47.70	1.185	21.14	51.38

But now from exergy analysis, it is found that, although, the COP was slightly high for the series configuration compared to that of the reverse parallel, but the exergy efficiency is relatively low and simultaneously, the total system irreversibility is high (in fact it is the highest among the three) for the series configuration compared to those of the reverse parallel. Therefore, among the two (series and reverse parallel), if higher COP is the sole criterion, the system designer can opt for the series configuration but at the cost of comparatively higher irreversible loss. On the other hand, if the total system losses are to be kept low, certainly the reverse parallel system is the system that needs to be preferred but with slight compromise in the COP value. That the COP (an outcome of energy analysis) alone is not a true performance measure of a cooling system is now evident from the results obtained from the exergy analysis. Exergy analysis, thus, helps in complete depiction of system performance characteristics which is not possible through energy analysis alone. It also offers flexibility at the hands of the system designer in decision making regarding selection of the proper configuration based on chosen criteria.

5.5.2 Effect of LPG temperature (T_{HPG}) on exergetic performance

Earlier in Chapter 4, variations of COP, component heat loads, SP power and solution concentrations (weak, medium and strong) were shown for the series, parallel and reverse parallel H$_2$O–LiCl VARS configurations with T_{LPG} by keeping T_{HPG} fixed at its corresponding optimum value. This was mainly done to show the optimal combination of T_{HPG} and T_{LPG} in the double effect VARS configurations for various test cases of fixed component temperatures. Now in this study, the exergy efficiency and total system irreversibility variation is presented for the same T_{LPG} range which is shown in Fig. 5.3a and Fig. 5.3b. From Fig. 5.3a, it is seen that it is not only the COP but also the exergy efficiency that shows an increasing trend with T_{LPG} in all the systems under various test cases. On the other hand, the total system irreversibility decreases with increasing T_{LPG} as expected.

These results of exergy efficiency and total system irreversibility now confirms that the optimal combinations of T_{HPG} and T_{LPG} corresponding to various cases of fixed component temperatures which were earlier obtained from energetic point of view for

the double effect H$_2$O–LiCl VARS configurations, now also hold well from the exergetic point of view. However, as reported in Chapter 4, the upper T_{LPG} limit is fixed due to maximum solution concentration which otherwise exceeds the 50% wt. limit. The lower bound of T_{LPG} is also set by the mass balance criterion. The total system irreversibility decreases with increasing T_{LPG} due to reduction in irreversible losses in majority of the components at higher T_{LPG}. This is specifically shown for Case 1 in Table 5.5 (a–b) for all the three double effect VARS configurations.
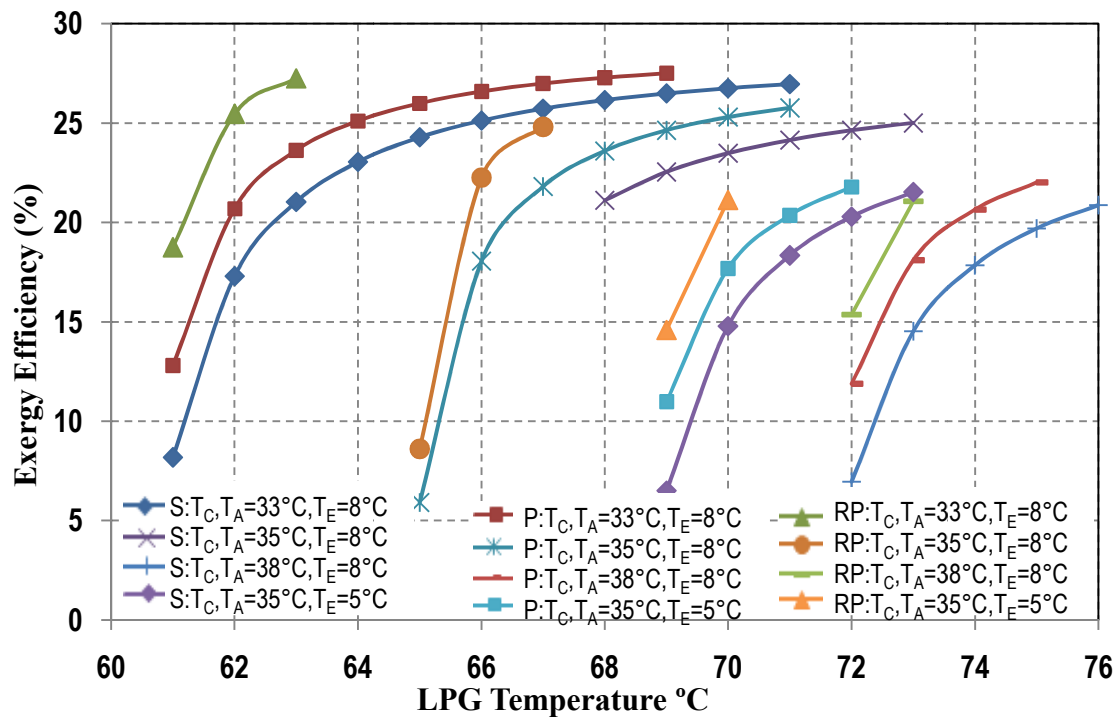

Fig. 5.3a: Exergy efficiency variation with T_{LPG} at fixed T_{HPG} for the series, parallel and reverse parallel configurations respectively [T_{HPG} fixed at (i) 105°C, 106°C and 102°C during Case 1, (ii) 109°C, 109°C and 108°C during Case 2 (iii) 116°C, 116°C and 115°C during Case 3 (iv) 112°C, 113°C and 112°C during Case 4]
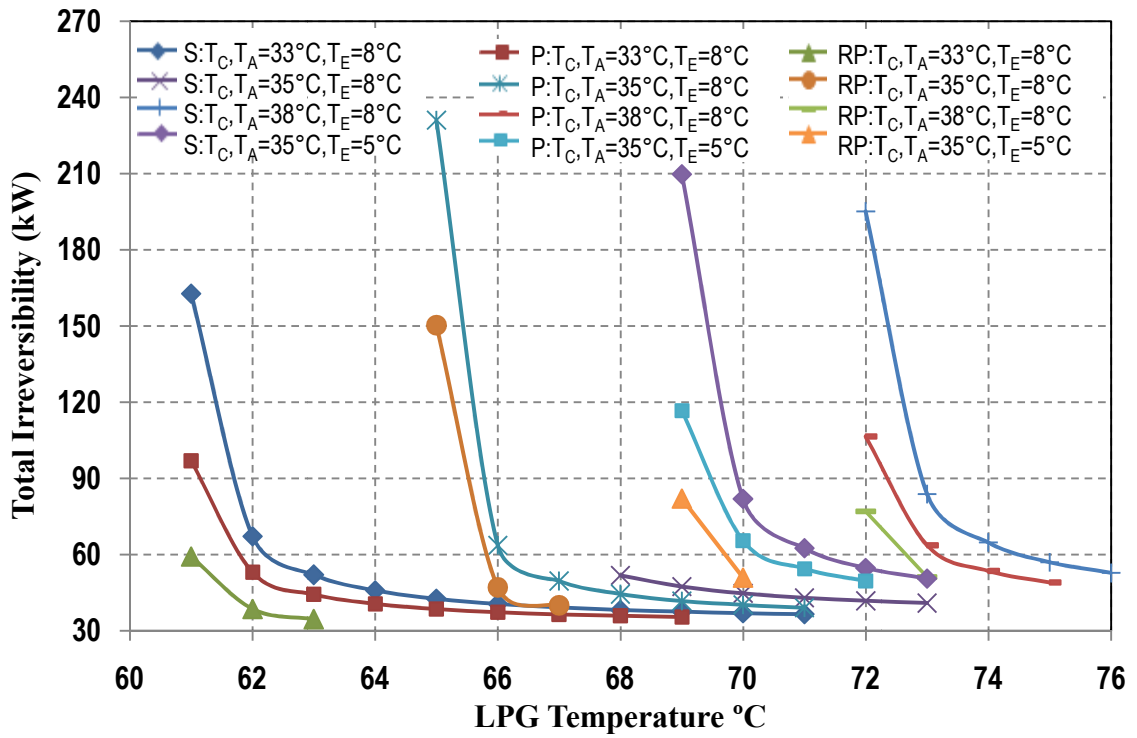
Fig. 5.3b: Total irreversibility variation with T_{LPG} at fixed T_{HPG} for the series, parallel and reverse parallel configurations respectively [T_{HPG} fixed at (i) 105°C, 106°C and 102°C during Case 1, (ii) 109°C, 109°C and 108°C during Case 2 (iii) 116°C, 116°C and 115°C during Case 3 (iv) 112°C, 113°C and 112°C during Case 4]

Table 5.5a: Component wise irreversibility (in kW) variation with T_{LPG} (T_{HPG} fixed at it optimal value) for Case 1 (Series)

T_{LPG}	$\dot{I}_{HPG}$	$\dot{I}_{LPG}$	$\dot{I}_C$	$\dot{I}_E$	$\dot{I}_A$	$\dot{I}_{SHE1}$	$\dot{I}_{SHE2}$	$\dot{I}_{ExV1}$	$\dot{I}_{ExV2}$	$\dot{I}_{ExV3}$	$\dot{I}_{ExV4}$	$\dot{I}_{ExV5}$	$\dot{I}_{SP1}$	$\dot{I}_{SP2}$
Series: T_{HPG} =105°C, T_C = T_A =33°C and T_E =8°C													
61	27.43	3.27	11.36	5.84	18.58	26.03	73.26	0.69	0.00	0.38	0.79	-	0.31	-
62	11.17	4.92	23.33	5.84	11.09	7.88	20.50	0.69	0.00	0.21	0.17	-	0.09	-
63	8.69	4.25	25.13	5.84	10.56	5.00	12.05	0.69	0.00	0.01	0.49	-	0.05	-
64	7.76	4.15	25.78	5.84	10.60	3.83	8.60	0.69	0.00	0.01	0.08	-	0.04	-
65	7.31	3.64	26.08	5.84	10.88	3.20	6.73	0.69	0.01	0.01	0.05	-	0.03	-
66	7.09	3.08	26.21	5.84	11.25	2.81	5.55	0.69	0.00	0.01	0.04	-	0.02	-
67	6.97	2.50	26.27	5.84	11.66	2.56	4.74	0.69	0.00	0.03	0.04	-	0.02	-
68	6.93	1.94	26.27	5.84	12.13	2.37	4.15	0.69	0.00	0.01	0.02	-	0.02	-
69	6.92	1.36	26.24	5.84	12.55	2.24	3.71	0.69	0.00	0.06	0.03	-	0.02	-
70	6.95	0.81	26.19	5.84	13.06	2.13	3.36	0.69	0.00	0.01	0.02	-	0.02	-
71	7.00	0.24	26.13	5.84	13.52	2.06	3.07	0.69	0.02	0.03	0.02	-	0.01	-

Table 5.5b: Component wise irreversibility (in kW) variation with T_{LPG} (T_{HPG} fixed at it optimal value) for Case 1 (Parallel and Reverse parallel)

T_{LPG}	$\dot{I}_{HPG}$	$\dot{I}_{LPG}$	$\dot{I}_C$	$\dot{I}_E$	$\dot{I}_A$	$\dot{I}_{SHE1}$	$\dot{I}_{SHE2}$	$\dot{I}_{ExV1}$	$\dot{I}_{ExV2}$	$\dot{I}_{ExV3}$	$\dot{I}_{ExV4}$	$\dot{I}_{ExV5}$	$\dot{I}_{SP1}$	$\dot{I}_{SP2}$
Parallel: T_{HPG} =106°C, $T_C=T_A$=33°C and T_E=8°C														
61	14.39	8.38	2.63	5.84	16.87	22.70	23.51	0.69	0.97	0.06	0.20	0.16	0.43	-
62	8.43	6.36	3.13	5.84	11.32	8.02	8.26	0.69	0.81	0.02	0.03	0.05	0.14	-
63	7.48	5.28	3.23	5.84	10.71	5.05	5.16	0.69	0.75	0.02	0.04	0.03	0.07	-
64	7.27	4.38	3.28	5.84	10.80	3.75	3.82	0.69	0.69	0.03	0.01	0.02	0.05	-
65	7.30	3.50	3.31	5.84	11.13	3.04	3.07	0.69	0.65	0.01	0.02	0.01	0.04	-
66	7.46	2.65	3.33	5.84	11.56	2.61	2.59	0.69	0.60	0.01	0.01	0.01	0.03	-
67	7.69	1.77	3.35	5.84	12.04	2.29	2.25	0.69	0.56	0.00	0.01	0.01	0.02	-
68	7.97	0.91	3.37	5.84	12.54	2.05	2.00	0.69	0.51	0.00	0.00	0.01	0.02	-
69	8.29	0.03	3.38	5.84	13.05	1.88	1.81	0.69	0.47	0.00	0.01	0.01	0.02	-
Reverse Parallel: T_{HPG} =102°C $T_C=T_A$=33°C and T_E=8°C														
61	5.90	5.49	2.61	5.84	12.60	12.99	12.41	0.69	0.75	0.00	0.00	-	0.03	0.01
62	2.93	2.63	3.02	5.84	10.55	4.59	7.88	0.69	0.55	0.00	0.00	-	0.01	0.00
63	2.92	0.19	3.10	5.84	11.24	2.96	7.19	0.69	0.41	0.00	0.00	-	0.01	0.00

5.5.3 Effect of distribution ratio (*D)* on exergetic performances of the double effect parallel and reverse parallel systems

The effect of distribution ratio '*D*' on solution concentrations, components' heat load, pressure and COP of the double effect parallel and reverse parallel configurations was presented in Chapter 4. In Chapter 4, it was found that the COPs of the double effect parallel and reverse parallel systems are usually more at low distribution ratio. However, there is a limit beyond which *D* cannot be lowered due to the maximum solution concentration (X_8) exceeding the 50% wt. limit. These lower limits of *D*'s for the parallel and reverse parallel systems were identified and reported in Chapter 4 for various cases. The exergy based results are now presented in this study for the same range of *D* for the double effect parallel and reverse parallel configurations. The exergy efficiency variation with *D* is shown in Fig. 5.4a while the total system irreversibility variation is shown in Fig. 5.4b. With increase in *D*, the exergy efficiency decreases in a similar manner as COP does in Chapter 4. When COP and exergy efficiency are less at higher *D*, it is obvious that the total system irreversibility will be more and this is what is exactly depicted in Fig. 5.4b.

The total system irreversibility increases with increase in *D* in both the parallel and reverse parallel systems at different cases of fixed component temperatures which is shown in Fig. 5.4b. With increase in *D*, the irreversible losses in the LPG, condenser, SHE I and SHE II show significant increase, both in the parallel as well as reverse parallel system and therefore, the total system irreversibility increases at higher *D*. The results of component irreversibility variation with *D* are shown in Table 5.6. With increase in *D*, however, the HPG and absorber irreversibility decreases but overall it shows an increase in total irreversibility at higher *D* due to increase in irreversibility in the other components.

Fig. 5.4a: Exergy efficiency variation with distribution ratio (D) at fixed T_{HPG} and T_{LPG} for the parallel and reverse parallel configurations respectively [(i) T_{HPG} fixed at 106°C and 102°C; T_{LPG} fixed at 69°C and 63°C during Case 1, (ii) T_{HPG} fixed at 109°C and 108°C; T_{LPG} fixed at 71°C and 67°C during Case 2, (iii) T_{HPG} fixed at 116°C and 115°C; T_{LPG} fixed at 75°C and 73°C during Case 3, (iv) T_{HPG} fixed at 113°C and T_{LPG} fixed at 72 for the parallel system during Case 4 (v) T_{HPG} fixed at 106°C and 104°C; T_{LPG} fixed at 66°C and 65°C during the additional case (Case 5: $T_C = T_A = 33$°C, $T_E = 5$°C)]

Fig. 5.4b: Total irreversibility variation with distribution ratio (D) at fixed T_{HPG} and T_{LPG} for the parallel and reverse parallel configurations respectively [(i) T_{HPG} fixed at 106°C and 102°C; T_{LPG} fixed at 69°C and 63°C during Case 1, (ii) T_{HPG} fixed at 109°C and 108°C; T_{LPG} fixed at 71°C and 67°C during Case 2, (iii) T_{HPG} fixed at 116°C and 115°C; T_{LPG} fixed at 75°C and 73°C during Case 3, (iv) T_{HPG} fixed at 113°C and T_{LPG} fixed at 72 for the parallel system during Case 4 (v) T_{HPG} fixed at 106°C and 104°C; T_{LPG} fixed at 66°C and 65°C during the additional case (Case 5: $T_C = T_A = 33$°C, $T_E = 5$°C)]

Table 5.6: Component wise irreversibility (in kW) variation with D variation at fixed T_{HPG}, T_{LPG}, T_C, T_A and T_E

D	$\dot{I}_{HPG}$	$\dot{I}_{LPG}$	$\dot{I}_C$	$\dot{I}_E$	$\dot{I}_A$	$\dot{I}_{SHE1}$	$\dot{I}_{SHE2}$	$\dot{I}_{ExV1}$	$\dot{I}_{ExV2}$	$\dot{I}_{ExV3}$	$\dot{I}_{ExV4}$	$\dot{I}_{ExV5}$	$\dot{I}_{SP1}$	$\dot{I}_{SP2}$
Parallel: T_{HPG} =106°C, T_{LPG} =69°C, $T_C = T_A$ =33°C and T_E =8°C														
0.50	8.29	0.03	3.38	5.84	13.05	1.88	1.81	0.69	0.47	0.00	0.01	0.01	0.02	-
0.55	7.72	1.14	3.39	5.84	12.57	2.10	2.18	0.69	0.55	0.00	0.01	0.01	0.02	-
0.60	7.35	1.98	3.40	5.84	12.10	2.41	2.61	0.69	0.60	0.01	0.01	0.01	0.03	-
0.65	7.14	2.63	3.42	5.84	11.69	2.80	3.14	0.69	0.65	0.00	0.00	0.02	0.03	-
0.70	7.05	3.14	3.43	5.84	11.33	3.33	3.81	0.69	0.69	0.02	0.01	0.02	0.04	-
0.75	7.12	3.55	3.44	5.84	11.10	4.14	4.72	0.69	0.72	0.00	0.01	0.03	0.05	-
0.80	7.40	3.90	3.46	5.84	11.02	5.34	6.02	0.69	0.75	0.00	0.01	0.04	0.07	-
Reverse Parallel: T_{HPG} =102°C, T_{LPG} =63°C, $T_C = T_A$ =33°C and T_E =8°C														
0.50	2.92	0.19	3.10	5.84	11.24	2.96	7.19	0.69	0.41	0.00	0.00	-	0.01	0.00
0.55	2.29	0.57	3.11	5.84	11.25	3.04	7.92	0.69	0.43	0.00	0.00	-	0.01	0.00
0.60	1.70	0.88	3.12	5.84	11.26	3.13	8.65	0.69	0.45	0.00	0.00	-	0.01	0.00
0.65	1.15	1.12	3.13	5.84	11.28	3.22	9.38	0.69	0.46	0.00	0.00	-	0.01	0.00
0.70	0.61	1.32	3.14	5.84	11.29	3.32	10.12	0.69	0.48	0.00	0.00	-	0.01	0.00
0.75	0.09	1.49	3.15	5.84	11.30	3.41	10.87	0.69	0.49	0.00	0.00	-	0.01	0.00

5.5.4 Exergetic performance comparison between the double effect H_2O–LiCl and H_2O–LiBr systems

A performance comparison in terms of COP, component heat loads, solution concentrations was done earlier in Chapter 4 between the double effect H_2O–LiCl and H_2O–LiBr systems. It was found that the double effect H_2O–LiCl systems perform better in terms of COP than its H_2O–LiBr counterparts relatively at low T_{HPG} and T_{LPG} . In Chapter 4, it was also found that the upper limit of T_{LPG} is low in the double effect H_2O–LiCl systems compared to those of the H_2O–LiBr systems, hence the COP comparison was shown for the same lower range of T_{HPG} and T_{LPG} . Now here in this study, the comparison between the series, parallel and reverse parallel configurations of the two systems (H_2O–LiCl and H_2O–LiBr) is shown in terms of exergy efficiency, component and total system irreversibility. The exergetic performance comparison between the double effect H_2O–LiCl and H_2O–LiBr VARS configurations is shown in Table 5.7 (a–b) for Case 1 at fixed $T_C = T_A$=33°C and T_E=8°C. However, for better understanding and comparison, the COP values are also shown along with the exergy efficiency and irreversibility values.

Results in Table 5.7 (a–b) show that the exergy efficiencies of the double effect series, parallel and reverse parallel H_2O–LiCl VARS configurations are higher than those of the H_2O–LiBr systems for the selected range of T_{LPG} and T_{HPG} . Like in case of COP, now the exergy efficiency differences between the double effect H_2O–LiCl and H_2O–LiBr systems are also relatively more at lower T_{LPG} and T_{HPG} in all the three (series, parallel and reverse parallel) configurations. The difference in exergy efficiency between the two systems however reduces at higher T_{LPG} and T_{HPG} . Again, the exergy efficiency difference between the two systems is the maximum in the reverse parallel configuration. Further it is seen that the double effect H_2O–LiCl systems not only perform better in terms of COP and exergy efficiency, but the total system irreversibility is also less compared to their H_2O–LiBr counterparts in all the three flow configurations. Further, the difference between total system irreversibility of the H_2O–LiCl and H_2O–LiBr systems is relatively more at lower T_{LPG} and T_{HPG} . This irreversibility difference between the two systems however reduces with increasing T_{LPG} and T_{HPG} .

Table 5.7a: Performance comparison between $H_2O-LiCl$ and $H_2O-LiBr$ at $T_C=T_A=33°C$ and $T_E=8°C$ (Series and Parallel)

T_{HPG} (°C)	T_{LPG} (°C)	$H_2O-LiCl$			$H_2O-LiBr$		
		COP	η (%)	$\dot{I}_{tot}$ (kW)	COP	η (%)	$\dot{I}_{tot}$ (kW)
		Series			Series		
101	64	1.239	24.22	42.735	1.123	21.93	48.982
101	65	1.304	25.48	39.723	1.225	23.94	43.35
103	67	1.370	26.31	37.935	1.329	25.53	39.576
106	69	1.400	26.21	38.186	1.378	25.80	39.031
108	71	1.419	26.13	38.384	1.408	25.92	38.798
114	71	1.402	24.63	41.951	1.390	24.40	42.438
110	73	1.431	25.92	38.876	1.426	25.82	39.053
115	73	1.418	24.71	41.766	1.412	24.60	41.981
		Parallel			Parallel		
102	65	1.402	27.16	36.130	1.349	26.13	38.129
104	65	1.395	26.57	37.381	1.342	25.53	39.517
106	65	1.389	26.00	38.617	1.334	24.96	40.840
106	67	1.442	26.99	36.541	1.418	26.54	37.383
108	67	1.436	26.45	37.690	1.412	25.99	38.595
108	69	1.464	26.96	36.595	1.454	26.76	36.955
110	69	1.460	26.44	37.710	1.449	26.24	38.083
112	69	1.455	25.95	38.799	1.444	25.74	39.221

Table 5.7b: Performance comparison between $H_2O-LiCl$ and $H_2O-LiBr$ at $T_C = T_A = 33°C$ and $T_E = 8°C$ (Reverse parallel)

T_{HPG} (°C)	T_{LPG} (°C)	$H_2O-LiCl$			$H_2O-LiBr$		
		COP	η (%)	$\dot{I}_{tot}$ (kW)	COP	η (%)	$\dot{I}_{tot}$ (kW)
		Reverse Parallel			Reverse Parallel		
97	62	1.333	27.04	35.222	1.117	22.66	45.935
99	62	1.325	26.39	36.604	1.104	21.97	47.933
101	62	1.317	25.76	37.987	1.091	21.32	50.063
103	62	1.310	25.16	39.370	1.078	20.70	52.113
102	63	1.406	27.25	34.535	1.343	26.02	37.452
106	63	1.395	26.12	36.942	1.328	24.85	40.208
110	63	1.384	25.08	39.336	1.313	23.77	42.917

The reason for not showing performance comparison for T_{LPG} above certain limiting value in case of H_2O–LiCl systems was explained earlier in Chapter 4. Therefore, the present exergetic performance comparison is also shown for the same combinations of T_{LPG} and T_{HPG}. Moreover it is shown only for Case 1 at fixed $T_C = T_A$ =33°C and T_E =8°C because among all the four various cases, the highest energetic and exergetic performances are obtained during Case 1 in all the three VARS configurations.

As far as the double effect H_2O–LiBr VARS configurations are concerned, it is possible to obtain better performance, in terms of COP, exergy efficiency and irreversibility, from the double effect H_2O–LiBr VARS configurations if these systems are operated at higher T_{LPG}. In fact, double effect H_2O–LiBr systems can be operated over a wide range of T_{LPG} because the crystallization conditions are not so stringent like in the H_2O–LiCl VARS configurations. Say for example, the double effect H_2O–LiBr series configuration, if operated at T_{LPG} =80°C and T_{HPG} =120°C by maintaining the other component temperatures fixed at Case 1 ($T_C = T_A$=33°C and T_E =8°C), the weak solution concentration (X_{15}) at LPG exit would be 0.613. Further it would give a COP of 1.437 with corresponding exergy efficiency of 24.16% and total irreversibility of 43.16 kW. This COP value is certainly higher than the maximum possible COP (1.428) obtained from the H_2O–LiCl series configuration with T_{LPG} =71°C and T_{HPG} =105°C and other component temperatures fixed at Case 1. However, the advantage with in the H_2O–LiCl series configuration is that the corresponding exergy efficiency is high (26.96%) and total irreversibility is also low (36.59 kW) compared to those of the H_2O–LiBr series configuration. As indicated in Chapter 4, it can again be mentioned that the double effect H_2O–LiCl VARS operation would not be possible at T_{LPG} =80°C and T_{HPG} =120°C if the other component temperatures are fixed at $T_C = T_A$=33°C and T_E =8°C. This is because the maximum solution concentration (X_{15}) in the series H_2O–LiCl VARS configuration will exceed 50% wt. limit leading to increased risk of crystallization. System operation of the double effect H_2O–LiCl VARS configurations at higher T_{LPG} can be made possible by simultaneously increasing the condenser and absorber temperatures or by lowering the evaporator temperature and D (in case of parallel and reverse parallel systems). However, in that case, the system performance will deteriorate; it will not be possible to

obtain higher COP and exergy efficiency and moreover, the irreversible losses in the systems will also increase.

Although many details regarding performance comparison of the H_2O–LiCl and H_2O–LiBr operated double effect VARS configurations were found out but from the above analysis it was not clear as to how much exergy was supplied to the systems and how much was finally available as output. In order to understand the details regarding exergy inflow, outflow and losses in the three double effect systems and also to investigate the difference between H_2O–LiCl and H_2O–LiBr in terms of exergy flow; the exergy flow diagrams are drawn which are shown in Fig. 5.5 (a–b), Fig. 5.6 (a–b) and Fig. 5.7 (a–b) respectively for the double effect series, parallel and reverse parallel systems, separately for H_2O–LiCl and H_2O–LiBr at some fixed components' temperatures.

From the Fig. 5.5a and Fig. 5.5b, it was observed that in the H_2O–LiCl and H_2O–LiBr operated double effect series flow configuration, there is not much difference in the exergy input and exergy losses that occurred in different VARS components. Comparatively, the exergy losses in the HPG and LPG were more while in the absorber, condenser, SHE–I and SHE–II; the exergy losses were relatively less in the H_2O–LiCl operated system compared to their values in the H_2O–LiBr counterpart. The other unaccounted exergy losses were also slightly less in the H_2O–LiCl operated double effect series flow system. This was also evident from the results shown in Table 5.7a that the total exergy loss (irreversibility) was relatively less in the H_2O–LiCl operated system compared to that of the H_2O–LiBr for almost the same exergy output of 15.33 kW from both the systems. In fact, the exergy output was the same in all the double effect systems for both H_2O–LiCl and H_2O–LiBr.

Similar observations were made also in the H_2O–LiCl and H_2O–LiBr operated double effect parallel configurations. However compared to the series flow, the exergy inputs in the two systems were less because of lower HPG and LPG temperatures and the exergy input in the H_2O–LiCl based system was little less compared to that of H_2O–LiBr. Further due to slightly lower HPG and LPG temperatures in the parallel system, the exergy losses in some components and the total exergy losses were comparatively less compared to the series both in the H_2O–LiCl and H_2O–LiBr operated systems.

In double effect reverse parallel system however a slightly different observations were made at the chosen component temperatures. The exergy input in case of the H_2O-LiCl system was 2.66 kW less compared to that of the H_2O-LiBr. This difference in system exergy input with H_2O-LiCl and H_2O-LiBr in the series and parallel system was however less than 1 kW. The HPG, LPG and SHE–II exergy losses which were more with H_2O-LiCl in the series and parallel flow double effect systems were also found less in the double effect reverse parallel system compared to those with H_2O-LiBr. In the condenser also, the exergy loss was slightly more for the H_2O-LiCl operated system. However in the absorber and SHE–I, and particularly in the SHE–I, the exergy loss with the H_2O-LiCl operated system was significantly less. This was the reason that finally the total component exergy loss was less for H_2O-LiCl compared to H_2O-LiBr (refer Table 5.7b) Further, it was observed that compared to the series and parallel, in the reverse parallel system, the other unaccounted exergy loss was little more for both H_2O-LiCl and H_2O-LiBr operated systems. Most interestingly, the evaporator exergy loss (5.84 kW) was the same in all the double effect systems (series, parallel and reverse parallel) for both H_2O-LiCl and H_2O-LiBr.
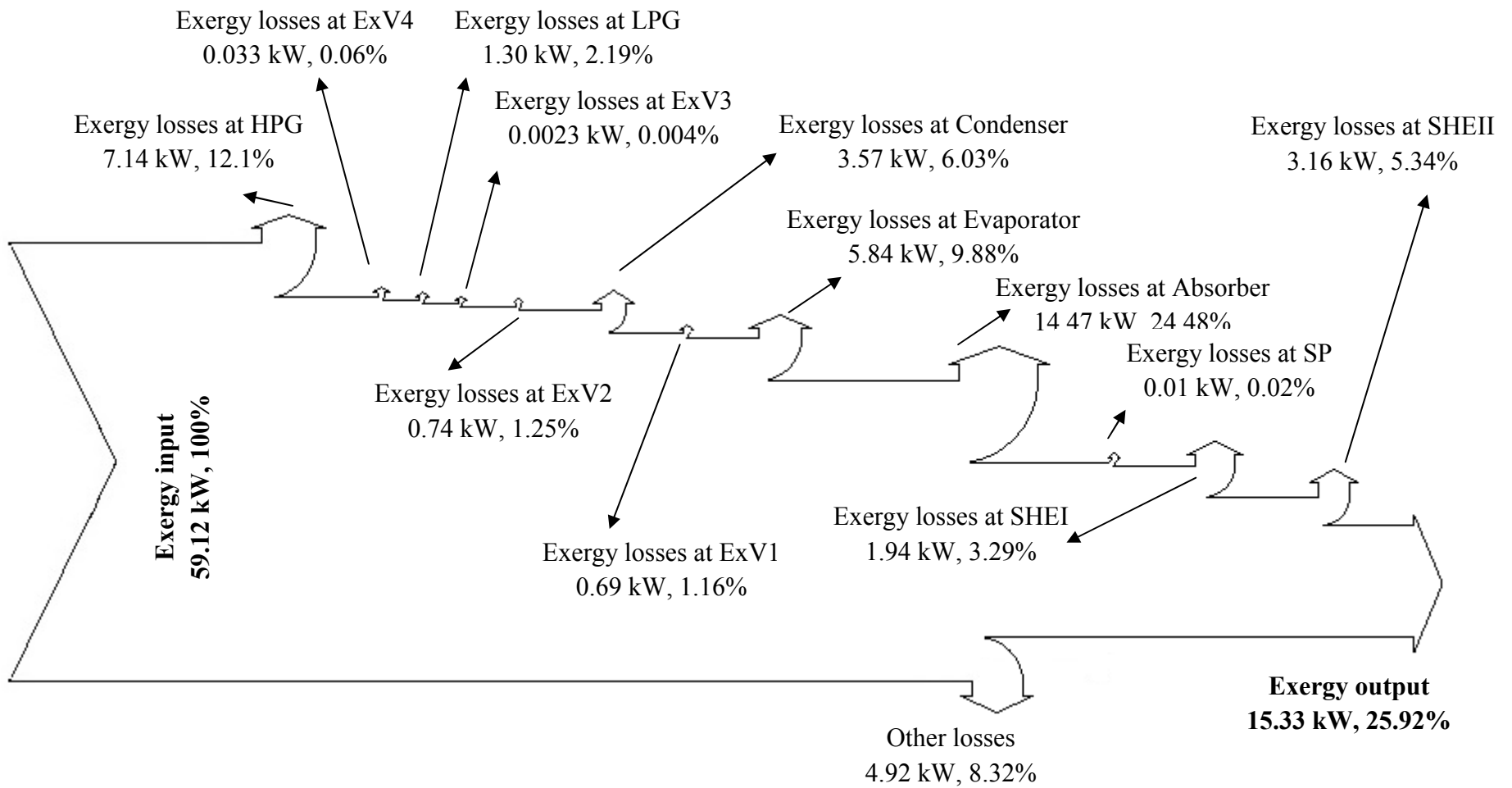
Fig. 5.5a: Exergy flow diagram of the double effect series flow H_2O–LiCl system at T_G=110ºC, T_{LPG}=73ºC, T_C=33ºC, T_A=33ºC and T_E=8ºC
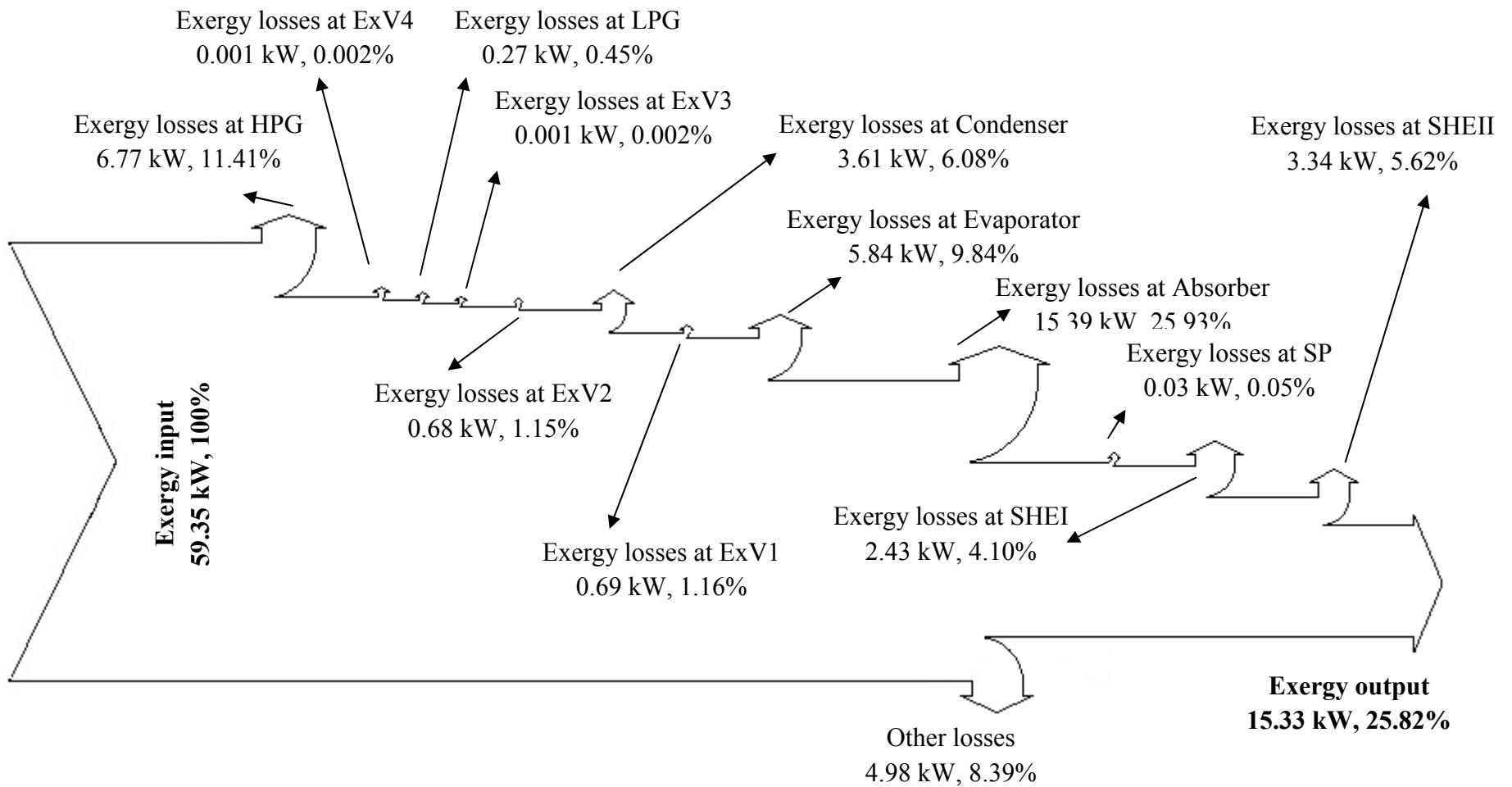
Fig 5.5b: Exergy flow diagram of the double effect series flow H$_2$O–LiBr system at T_G=110ºC, T_{LPG}=73ºC, T_C=33ºC, T_A=33ºC and T_E=8ºC
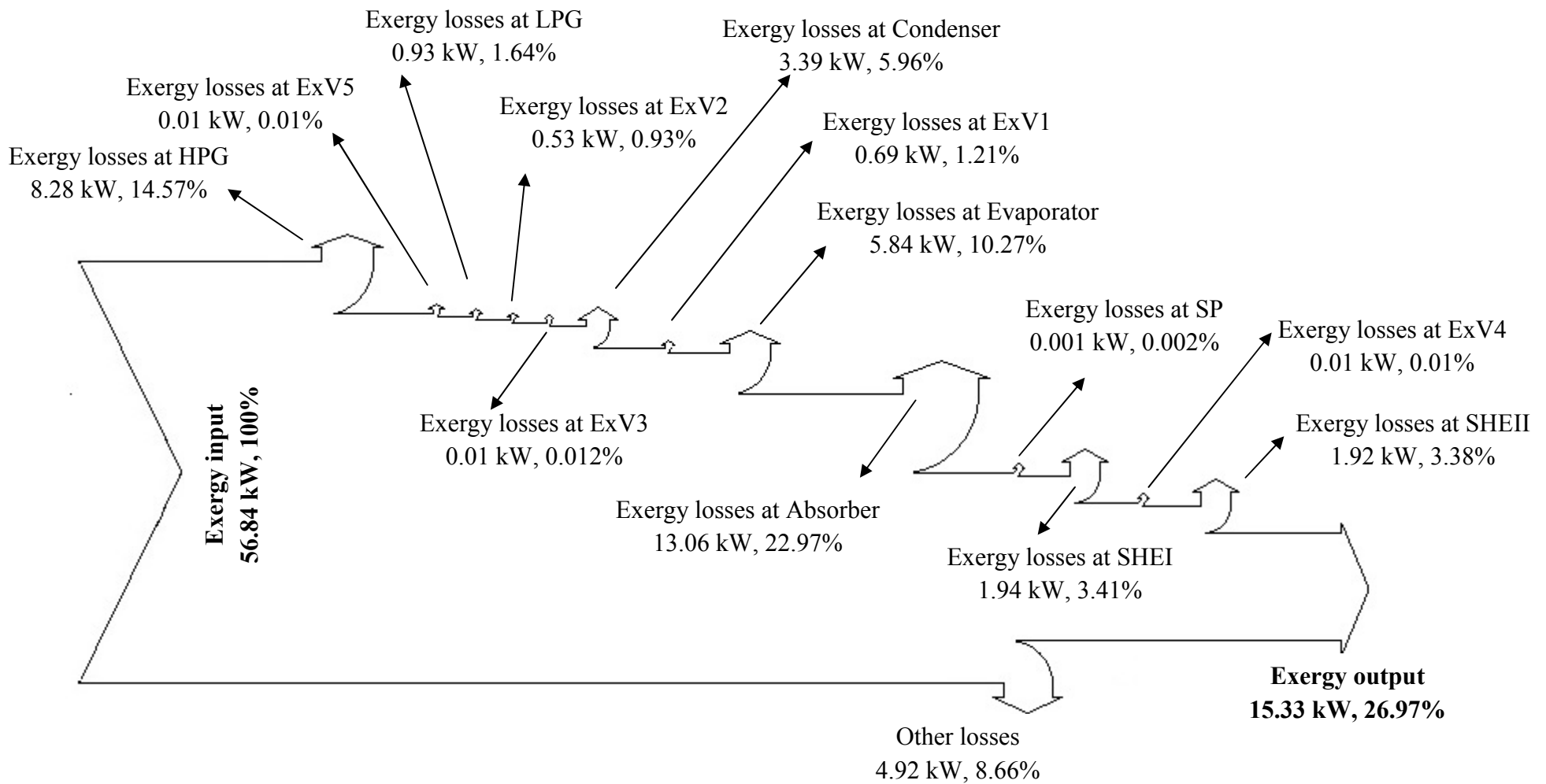
Fig. 5.6a: Exergy flow diagram of the double effect parallel flow H_2O–LiCl system at T_G=108ºC, T_{LPG}=69ºC, T_C=33ºC, T_A=33ºC, T_E=8ºC and D = 0.50

230
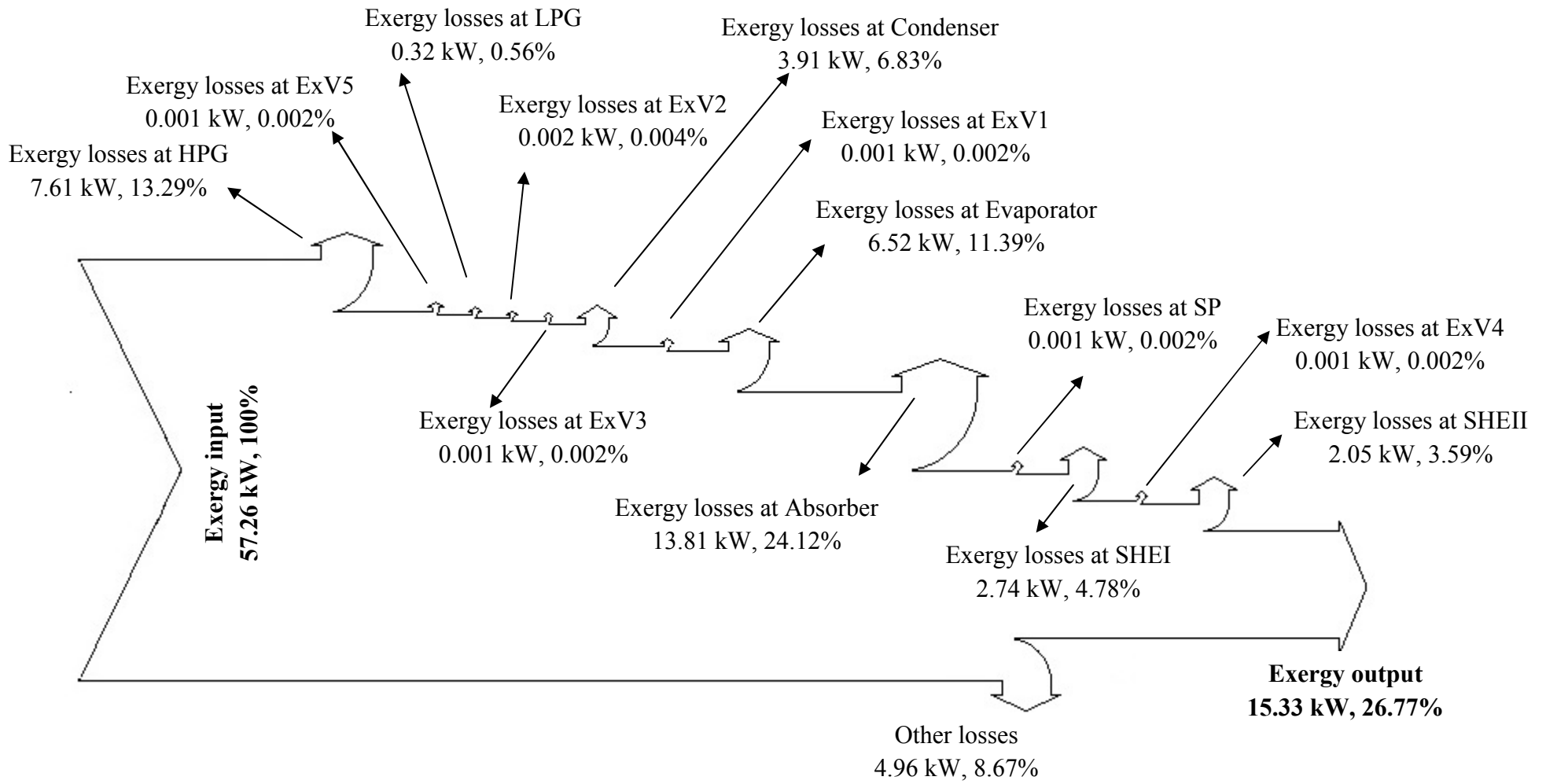
Fig. 5.6b: Exergy flow diagram of the double effect parallel flow H_2O–LiBr system at T_G=108ºC, T_{LPG}=69ºC, T_C=33ºC, T_A=33ºC, T_E=8ºC and $D = 0.50$

Exergy losses at LPG
0.19 kW, 0.34%

Exergy losses at ExV4
0.0001 kW, 0.002%

Exergy losses at Condenser
3.19 kW, 5.67%

Exergy losses at HPG
2.92 kW, 5.19%

Exergy losses at SP2
0.010

Exergy losses at ExV3
0.0001 kW, 0.002%

Exergy losses at ExV1
0.69 kW, 1.23%

Exergy losses at Absorber
11.48 kW, 20.42%

Exergy losses at Evaporator
5.84 kW, 10.39%

Exergy losses at SP1
0.01 kW, 0.02%

Exergy input
56.23 kW, 100%

Exergy losses at SHEII
7.19 kW, 12.79%

Exergy losses at SHEI
2.96 kW, 5.26%

Exergy losses at ExV2
0.41 kW, 0.73%

Exergy output
15.33 kW, 27.25%

Other losses
6.02 kW, 10.70%

Fig. 5.7a: Exergy flow diagram of the double effect reverse parallel flow H$_2$O–LiCl system at T_G=102ºC, T_{LPG}=63ºC, T_C=33ºC, T_A=33ºC, T_E =8ºC and D = 0.50

232

Exergy losses at LPG
0.572 kW, 0.971%

Exergy losses at ExV4
0.0001 kW, 0.002%

Exergy losses at HPG
5.82 kW, 9.87%

Exergy losses at SP2
0.0001 kW, 0.002%

Exergy losses at Condenser
3.16 kW, 5.34%

Exergy losses at ExV3
0.0001 kW, 0.002%

Exergy losses at ExV1
0.69 kW, 1.17%

Exergy losses at Absorber
12.07 kW, 20.50%

Exergy losses at Evaporator
5.84 kW, 9.92%

**Exergy input
58.89 kW, 100%**

Exergy losses at SP1
0.0001 kW, 0.002%

Exergy losses at SHEII
3.87 kW, 6.57%

Exergy losses at SHEI
4.97 kW, 8.44%

Exergy losses at ExV2
0.46 kW, 0.79%

**Exergy output
15.33 kW, 26.02%**

Other losses
6.12 kW, 10.39%

Fig. 5.7b: Exergy flow diagram of the double effect reverse parallel flow H_2O–LiBr system at T_G=102ºC, T_{LPG}=63ºC, T_C=33ºC, T_A=33ºC, T_E =8ºC and D = 0.50

233

5.6 Summary

In this Chapter, the exergetic performances of double effect H_2O–LiCl VARS configurations (series, parallel and reverse parallel) are evaluated by investigating the effect of components' temperature and distribution ratio (in case of parallel and reverse parallel system) on exergy efficiency and irreversibility. Further, in this study, the performances of the double effect H_2O–LiCl and H_2O–LiBr VARS configurations are compared from exergetic point of view under identical operating conditions. The following important observations are made from this exergy analysis.

- The optimal combinations of T_{HPG} and T_{LPG} which were found earlier from energy analysis in Chapter 4, also remain valid in this Chapter. These operating conditions of the double effect H_2O–LiCl VARS configurations with respect to maximum COPs (in Chapter 4) and maximum exergy efficiencies now in this Chapter are almost identical in all the systems except in Case 1 at $T_C = T_A = 33°C$ and $T_E = 8°C$ where a little mismatch is observed in T_{HPG} and T_{LPG} values for the series and parallel configurations.

- Like the COP in Chapter 4, now the exergy efficiency in this study also changes in a similar pattern with T_{HPG} and T_{LPG} in all the three double effect H_2O–LiCl VARS configurations under various cases of fixed component temperatures.

- The operating conditions of the double effect H_2O–LiCl VARS configurations corresponding to the maximum exergy efficiency and the minimum total system irreversibility are identical.

- In all the three double effect VARS configurations, the best performance earlier in terms of COP in Chapter 4 and now in terms of exergy efficiency and irreversibility in this Chapter are found during Case 1.

- Among the three double effect H_2O–LiCl VARS configurations (series, parallel and reverse parallel), the parallel configuration provides the best performance showing higher COP and higher exergy efficiency and lower total system irreversibility in all the four test cases. This is the scenario particularly at higher T_{LPG} and T_{HPG} values of the selected range. At certain lower range of T_{LPG} and T_{HPG} however, the series flow configuration provides higher exergy efficiency and lower system irreversibility than the parallel system.

234

- In the series and parallel systems, during Case 1 and Case 2, although the COPs are found more for the series configuration compared to the reverse parallel, but the corresponding exergy efficiencies are less while the total system irreversibility values are more. One would have left with an impression and certainly would have preferred the series configuration based on higher COP value, but now from exergy analysis, it has been found that energy analysis alone is not sufficient and exergy is needed in order to depict the complete system performance characteristics.

- In the double effect parallel and reverse parallel configurations, the exergy efficiency variation with the distribution ratio 'D' shows almost the similar trend of variation with COP, shown earlier in Chapter 4. Thus, the exergy efficiencies of the double effect parallel and reverse parallel systems are found to be maximum with corresponding minimum total system irreversibility values at the optimum D values identified earlier in Chapter 4 for these two systems under various cases of fixed component temperatures.

- The exergetic performance comparison between the double effect H_2O–$LiCl$ and H_2O–$LiBr$ VARS configurations under identical operating conditions (relatively at lower T_{LPG} and T_{HPG}) now confirms superior performance in respect of the double effect H_2O–$LiCl$ VARS configurations compared to those of the H_2O–$LiBr$ systems. Most importantly, higher COP and exergy efficiency are obtained from the double effect H_2O–$LiCl$ VARS configurations with corresponding lower total system irreversibility.

- From the results shown in Chapter 4 and now from the present exergy based results, it can be concluded that double effect H_2O–$LiCl$ VARS configurations can be preferred over double effect H_2O–$LiBr$ systems in applications requiring low T_{LPG} and T_{HPG} for obtaining better system performance. Use of low temperature heat sources such as steam, solar energy (solar water heaters, solar ponds etc.), geothermal and other waste heat sources (hot liquid and water from industrial processes, engine cooling water) could be vital in this regard. Further, depending on T_{LPG} and T_{HPG}, the proper double effect configuration be selected.

Bibliography

[1]   Ziegler, F., Kahn, R., Summerer, F., and Alefeld, G. Multi effect absorption chillers. *International Journal of Refrigeration,* 16: 301–311, 1993.

[2]   Farshi, L. G., Mahmoudi, S. M. S., Rosen, M. A., and Yari, M. A. Comparative study of the performance characteristics of double-effect absorption refrigeration systems. *International Journal of Energy Research*, 36:182–192, 2012.

[3]   Farshi, L. G., Mahmoudi, S. M. S., and Rosen, M. A. Analysis of crystallization risk in double effect absorption refrigeration systems. *Applied Thermal Engineering,* 31: 1712–1717, 2011.

[4]   Talukdar, K. and Gogoi, T. K. Exergy analysis of a combined vapor power cycle and boiler flue gas driven double effect water–LiBr absorption refrigeration system. *Energy Conversion and Management,* 108: 468–477, 2016.

[5]   Patek, J. and Klomfar, J. Thermodynamic properties of the LiCl–H_2O system at vapour–liquid equilibrium from 273 K to 400 K. *International Journal of Refrigeration,* 31:287–303, 2008.

[6]   Wagner, W., Cooper, J. R., Dittmann, A., Kijima, J., Kretzschmar, H. J., Kruse, A., et al. The IAPWS Industrial Formulation 1997 for the thermodynamic properties of water and steam. *Journal of Engineering, Gas Turbine Power,* 122:150–81, 2000.